Semi-Automatic Medical Syringe Pump Development: Interface, Control, Alarm, and Feedback

Kevin Nicholas Tanex[1], Megantara Pura[2]

[1,2] Electrical Engineering, Universitas Multimedia Nusantara, Tangerang, Indonesia

[1]kevin.tanex@gmail.com, [2]megantara.pura@umn.ac.id

Abstract— **The syringe pump is used to inject liquids for a long period of time and on a small volume scale. The presence of air inside the hose whilst injection into the human body is dangerous. Early detection can be done using a bubble sensor. The SPICAF is equipped with a gearbox capable of injecting long-term injections on a small scale, and a bubble sensor capable of detecting air by comparing light intensity on a clear hose which automatically notifies the user if dangerous conditions occur. The SPICAF is successfully designed, developed, and tested to WHO specifications. It's injection has 98% accuracy and is able to detect air bubbles properly.**

Index Terms— **automatic; bubble sensor; gearbox; injection; injection pump.**

I. INTRODUCTION

Some diseases experienced by a patient require regular treatment and need to be observed by health workers gradually and periodically [1]. In one treatment process, health workers need to periodically give medicine to patients, it can be in the form of solid or liquid drugs [2]. One way to give liquid medicine is by injection method. The injection process transfers liquid drugs into the human bloodstream [3]. Drugs that are injected include insulin or other hormones, antibiotics, chemotherapy drugs, and pain relievers [4]. The injection method is usually done manually by health workers using injections or automatically using tools. One of the tools that can perform injection automatically is a syringe pump [5]. The automatic injection can lighten the workload while reducing the risk of inaccuracy by health workers [6]. During the injection process, the presence of air that enters the human bloodstream is called an anomaly of air embolism [7]. Embolism is a condition in which the presence of air in the blood circulation causes obstruction of blood flow [8]. Blood supply is blocked due to embolism can cause major human organs such as the brain, heart, and lungs to experience blood deficiency [9]. In the worst case, blood deficiency causes organ failure and death [10].

From the preceding context, this study aims to develop a syringe pump that can operate automatically and prevent air from entering the human blood circulation by detecting it before proceeding with the injection. Researcher chose to develop a syringe pump because the response time is more stable than peristaltic pumps and more affordable than pressure-driven pumps. Syringe pumps can perform injections on a very small scale, accurately, and at a specific speed. [11]. Previous study has developed a technique for detecting air inside human blood, employing a capacitive sensor method to identify bubbles, which was detected after the hemodialysis process [12]. Other research uses the triple modular redundancy (TMR) method in their sensors to make a fault tolerant air bubble detector [13]. The created syringe pump in this study takes a novel approach to the problem. It has a luxmeter-based bubble sensor module that detects bubbles in the injection hose and can take input from health staff so that it may operate autonomously. Sensor readings are used as feedback to be processed and notify health workers if there are problems during operation. The developed syringe pump system is called SPICAF (Syringe Pump: Interface, Control, Alarm, and Feedback). In conclusion, SPICAF is able to deliver injection accurately at given flowrate and is able to check for any air bubbles inside its hose.

II. RESEARCH METHOD

A. Design Concept

The process of making SPICAF follows the standard syringe pump specifications from WHO (World Health Organization) [14]. SPICAF is composed of hardware, electronic components, and software. The SPICAF structure is made of acrylic board and MDF (Medium-Density Fiberboard) which are connected using elbows and hinges. Some hardware components are made using a 3D (three-dimensional) printer while others are purchased. Electronic components include keypad, LCD (Liquid Crystal Display), LED (Light Emitting Diode), luxmeter BH1750 module, buzzer, stepper motor, stepper motor driver, microcontroller, micro SD (Secure Digital) card module, ATS (Automatic Transfer Switch), batteries,

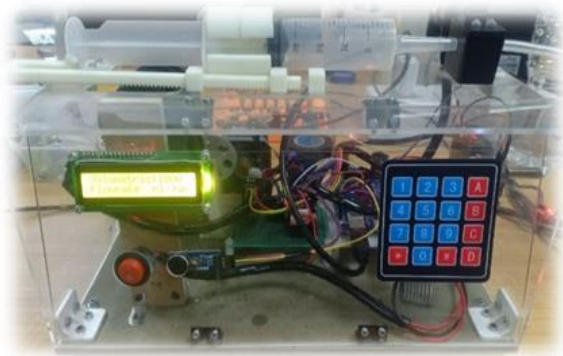adapter, and step-up module. The following are the results of the development of SPICAF.

Fig. 1. SPICAF Front View

From the design above, how to use SPICAF to be developed can be described as follows.
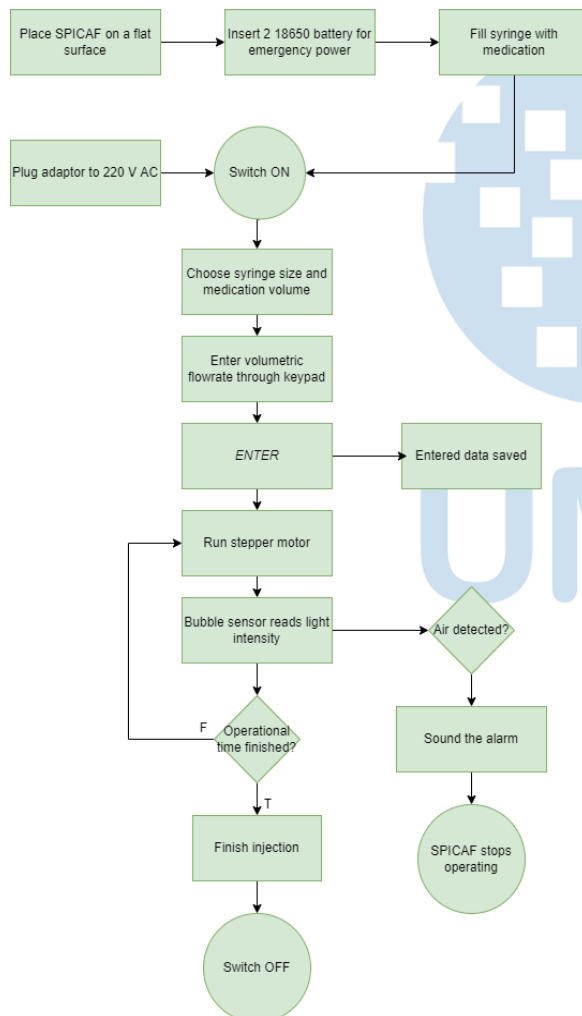

Fig. 2. SPICAF Flowchart

B. Subsystem

The SPICAF system consists of several subsystems connected to the microcontroller. The subsystem consists of hardware and electronic components, some of which are run using Arduino IDE (Integrated Development Environment)-based software.
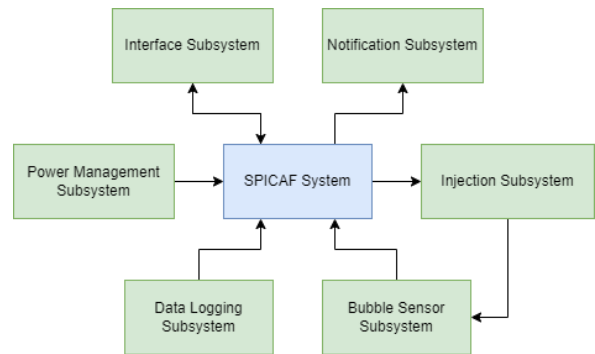

Fig. 3. Diagram of the subsystems on SPICAF

The interface subsystem interacts with the user through the 4x4 keypad and LCD components. This subsystem serves to receive user input and show the results of the input to the user.

The user notification subsystem functions to notify the condition of the SPICAF when operating, whether it is normal or experiencing problems. Notifications are notified via the LCD and buzzer.

The data logging subsystem is a subsystem that will store the input results and the results of calculations entered by the user into the micro-sd card via the micro SD card module.

The injection propulsion subsystem will drive the syringe to perform the injection. The driving component uses a stepper motor connected to a gearbox and rack and pinion which converts rotational motion into linear motion [15]. The stepper motor used is NEMA 17 which is controlled using the A4988 stepper motor driver. The reading of the rotational speed of the stepper motor uses a digital rotary encoder in rpm (rotation per minute).

The bubble sensor subsystem functions to detect air during the injection. Detection is done by comparing the difference in light intensity of the clear hose and the liquid-filled hose [16]. The light is emitted by the LED and measured by the BH1750 in a closed black box. Light intensity is in lux units.

With the subsystems above, SPICAF has some features and spesifications which fullfills some of the WHO standard criterias, includes:

- Automatic data logging
- Bubble detection
- Softstarter implementation
- Temporary back-up power
- User interface to receive and show input
- User notification with alarm sound not less than 45 dB
- Stepper motor rotation speed from 1 to 300 rpm, which translates to volumetric flowrate injection of 3600 nl/hour – 1080000 nl/hour

III. ANALYSIS

A. Bubble Sensor Subsystem

Air bubble sensor is used to detect the precence of air inside a vessel. Research [12] uses platinum plates to create the capacitor sensor. In their experiment, they used Dextran70 solution to simulate blood. Their sensor outputs certain voltage to detect the air bubbles. On the other hand, research [13] also uses capacitive sensor with TMR implementation. It incorporates a voting technique into the voter circuitry at the end of their sensors to guarantee that they all work together and get the same input signal. This ensures their air bubble detector is accurate and prevents sensor errors, especially if sensors fail to function properly.

The bubble sensor subsystem in this setup detects air by comparing the difference in light intensity when it is filled with air or liquid in a clear hose. The bubble sensor is positioned just after syringe's tip. In contrast to the previous studies, this setup merely employs LED, a black box, and a BH1750 luxmeter. Light is emitted by the LED. Light intensity is then measured by BH1750 sensor in lux unit [17] inside a black acrylic box measuring 2 x 4 x 3 cm^3. BH1750 is a digital ambient light sensor IC for I2C bus interface. Measurement of light intensity is carried out using a *millis()* based timer from the Arduino IDE. The measurement is carried out in a well-lit laboratory. The syringe hose is then filled with water or air as an experiment limitation.
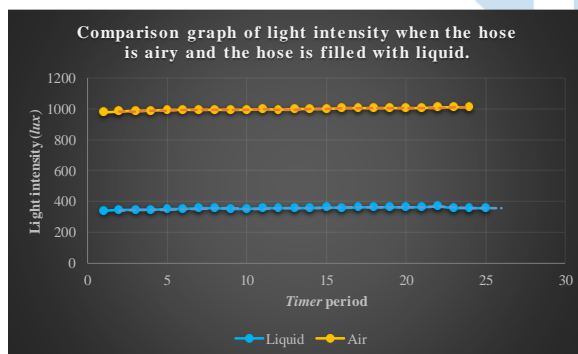

Fig. 4. Graph of measuring the intensity of light when the hose is airy and the hose is liquid

It is worth noting that the hose has a diameter of 5 mm. Outlier data is ignored from the statistical calculation of the data. In air condition, the data has a mean of 996,4132 lux with a maximum of 1009 lux, while in liquid condition, the mean is 355,1332 lux with a maximum of 365 lux. If sensor reads more than 365 lux, it indicates the existence of trapped tiny air bubbles during injection. By comparing these results, it is possible to deduce that as long as the bubble sensor detects a light intensity of less than 365 lux, the subsystem does not detect air and the SPICAF runs normally without any bubble inside its hose.

B. Injection Subsystem

The injector subsystem drives the injection via a gearbox-driven rack and pinion. The main source of movement is NEMA 17 stepper motor accompanied with a digital rotary encoder. Gear reduction of the gearbox is 1:562024. Rack and pinion do not affect gear reduction. With the gear reduction made, SPICAF is able to inject with a minimum resolution of 1 nl/hour (nanoliter) and a maximum resolution of 1 ml/hour (mililiter). This resolution is more than enough to qualify the spesifications by the WHO standars spesifications [14] which specifies the minimal flow rate range is 0.1 mL/hr.

The parameters and equation to calculate a formula and achieve injection succesfully is not specified in WHO standards. It is the developer's task to develop it. The formula to determine the required rpm for stepper motor to achieve the inputted flowrate is given below. Note that the user needs to input the flow rate in nL/hour. Since the formula finds rotation per minute, the nL/hour is converted to mL/minute first. The conversion from nL/hour to mL/minute is 1/60000000. To change the mL into into rotation, a ratio is needed based on the size of the syringe. Length of the syringe varies is ratioed with the stepper headgear size, in this case the headgear is 4,715 cm which is equal to 1 rotation of the headgear. Those are then applied to the formula:

$$rpm = \frac{flowrate * reduction\ gear\ ratio}{stepper\ rotation\ to\ syringe\ length\ ratio} * \frac{1}{6 * 10^7} \qquad (1)$$

One full rotation of the NEMA 17 stepper motor in formula (1) is equal to 200 steps with 1.8° step angle, which is equal to 360° [18]. Since the stepper motor library works by setting the speed in step/s, we need to convert rpm into step/s using the formula below:

$$\frac{step}{s} = (rpm * \frac{200}{60}) \qquad (2)$$

The injection subsystem features a soft starter implementation. The rotation speed of the stepper motor is measured using a digital rotary encoder. In addition to the rpm reading, the stepper motor performance was also measured when with and without an injection load until it reaches steady state. The experiment is run on 100 rpm, 200 rpm, and 300 rpm.

To determine the true accuracy of the instrument output, obtaining the actual output of the syringe and compare it to the entered data is necessary. However, it is difficult as there is no sensor capable of reading such small scale data for flowrate and volume. As a temporary solution, an alternative approach is to measure the stepper motor's rpm, provided that the gearbox and rack-pinion are ideal and computation . The expected outcome of the syringe injection process should be consistent with the stepper motor's rotation speed. Deductively, if the stepper motor is accurate, the injection process output is also accurate.
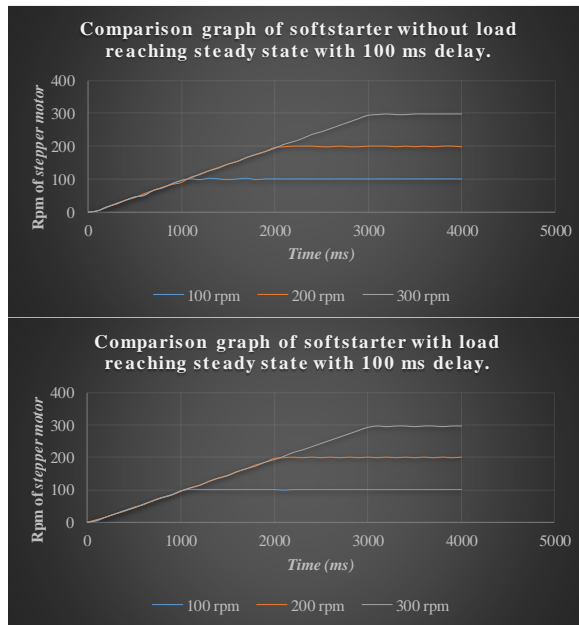
Fig. 5. Above: Graph of data measurement of the injection subsystem without load. Below: Graph of measurement data of the injection subsystem with the load

Measurements were made with a target rpm of 100 rpm (blue), 200 rpm (orange), and 300 rpm (green). The rpm reading by the encoder is obtained from the value of the phase *dt* (data)-pin to *clk* (clock)-pin [19] multiplied by two for each phase shift.

$$rpm = encoder * 2 \qquad (3)$$

Both measurement graphs use a soft starter to reach a steady state. The soft starting feature works by repeatedly adding a constant from 0 to the desired rpm until it is attained. Additions are made every 100 ms. The results of the subsystem data indicate the time required to reach the target rpm and the significance of the load on the rpm speed of the stepper motor. The digital rotary encoder data for measuring rpm is accurate according to the specified input. The error that occurs is based on the limitations of the encoder, which misses reading of 0-3 rpm points from the actual rpm as described in the datasheet [19]. To get the accuracy of the injection, we calculate the percentage error of the reading, which is

$$Percentage\ error = \frac{|True\ value - Measured\ value|}{True\ value} * 100\% \qquad (4)$$

The measured value of rpm after reaching steady state is often ±3 rpm of the actual value. Within 100 rpm to 300 rpm of inputs, the percentage error averages to ±2%. This formula from rpm reading to calculate accuracy is representative of the actual delivered liquid drug volume by the system with the rack and pinion part is considered ideal. According to WHO specifications [14], the volumetric flow rate accuracy with a common syringe should be ±5%. The SPICAF percentage error is ±2%, which passes the accuracy requirements.

The graph of the injection subsystem without and with load shows the presence or absence of injection does not affect the rpm of the stepper motor. The implementation of the soft starter also functions according to the intention where the stepper motor is run from 0 rpm to the target rpm. This implementation prevents stalling if the stepper motor directly runs at high rpm, because when the rpm is high, the torque produced by the stepper is low [20].

Soft starter time reaches steady state of 100 rpm in 1 second, 200 rpm in 2 seconds, and 300 rpm in 3 seconds. This is due to the addition of (+1) to the soft starter feature, which starts at 0 and has a delay of 100 ms each addition until the goal speed is reached. The given delay ensures that the encoder can read the soft starter rpm speed slowly and prevents current spikes from occurring in the A4988 driver when running the stepper motor. The time to reach steady state is not significant to the total operating time as the operating time usually runs in hours.

C. Interface Subsystem

The user interface subsystem interacts with the user via the keypad to receive input and the LCD to display the input. Each input, the LCD will refresh the screen to display the input. The number keys are used to enter numeric data, the C key to delete entries, and the D key to ENTER. Experiment limitations for this subsystem are the number keys and letter C and D. All output of the subsystem experiment is shown on the LCD.

Fig. 6. Top: Process of pressing keys on the keypad. Middle: Pressing the C key, the input is deleted and then ready to accept the new entry. Bottom: Receipt screen enters volumetric flowrate and enter numeric data

Volumetric flowrate entered in units of nL/hour. Based on the gear reduction of the injection propulsion subsystem, the minimum is 3600 nL/h and the maximum is 1080000 nL/h. Translated to motor rpm, the rotational speed reaches 1-300 rpm.

Based on the image of the test results, the subsystem was successfully operated according to its implementation objectives. The volumetric flowrate data entry only accepts numbers so that when the letters A, B, *, or # are pressed, they are not processed. The C button was successfully used to delete the input if the user entered incorrectly. The D key is successfully used to enter ENTER which will then be further processed by the system. Each time the button is pressed, the LCD successfully refreshes the screen to display the most recent input.

D. Notification Subsystem

The user notification subsystem plays a role in notifying users when a problem occurs. According to WHO specification standards, a minimum noise level of more than 45 dB (decibel) is required. SPICAF noise is generated by a passive buzzer. SPICAF notification noise was measured in decibels (dB) using the Android software Spectroid.
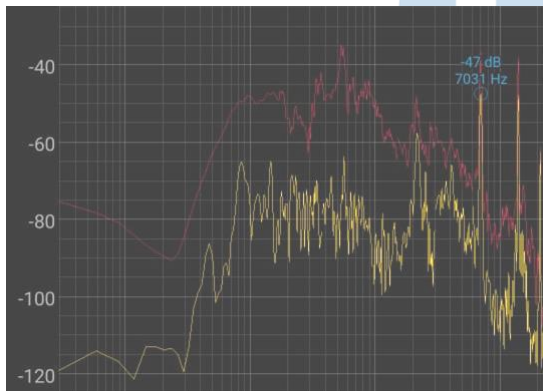

Fig. 7. Reading the buzzer noise using Spectroid

Noise measurements were taken at a 10 centimeter distance to mimic the user being near to the instrument. The noise measurement at an 8-meter distance depicts the user being outside of the room from the instrument. The experiment operates at a frequency range of 0 to 7500 Hz. Based on the limits stated above, the obtained data was shown in the graph below.
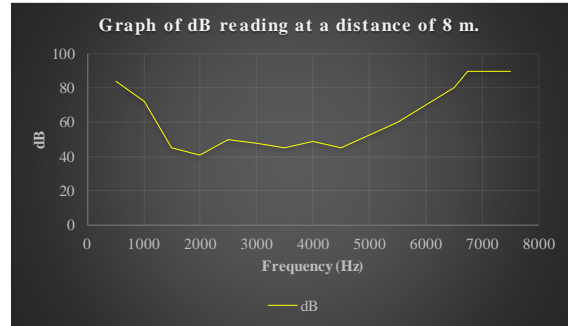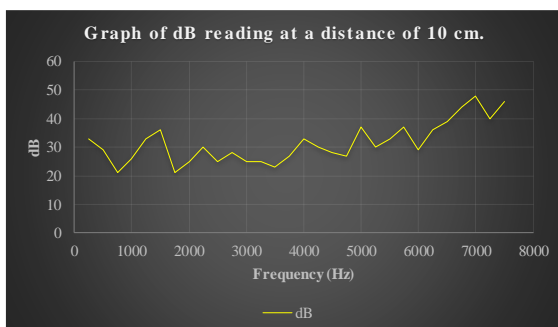

Fig. 8. Above: Buzzer noise measurements at a distance of 10 cm. Bottom: Buzzer noise measurements at a distance of 8 m

The graph of the data measurement shows the frequencies buzzer able to produce. The data read by Spectroid application shows that at distance of 10 cm, the buzzer reaches a noise of more than 45 dB after being more than equal to 7000 Hz (hertz), hence less than 7000 Hz noise produces less than 45 dB. For that, the buzzer will sound with a frequency of 7000 Hz.

For noise at a distance of 8 m, frequencies above 2000 Hz have reached more than 40 dB. When 7000 Hz the noise reaches 90 dB. At 1000-2000 Hz the noise is so disturbed by environmental noise that it becomes an outlier. Frequency of more than 2000 Hz is possibly affected by environmental noise.

E. Power Management Subsystem

The power manager subsystem (PMS) functions to supply power to the system. It ensures the system always have a backup power. The ATS transitions power from the adapter's AC (Alternating Current) source to the battery's DC (Direct Current) source when the AC power is not available [21]. The following pictures show the ATS operating conditions.

Fig. 9. Above: PMS state when using AC power adapter. Below: PMS state when using battery DC power

The truth table shows the PMS usage conditions when the AC adapter power is on, starting the battery usage and vice versa.

TABLE I. PMS TRUTH TABLE

ATS Truth Table	Adaptor	Battery
AC on	✓	✗
AC off	✗	✓

The truth table shows the PMS successfully delivered power between the AC adapter and the DC battery. When the AC power is off, the ATS pulls power from the battery. When AC power is available again, the ATS re-transitions the power to AC. Verification is done by checking the voltage on the adapter port MT36088 and battery port XL60099 when the AC condition is both available and inaccessible. This feature is partially achieved according to the intented specification following WHO standard [14].

The test results show, when making the transition, there is a delay. Delay arises from the use of relay logic, which is not an instantaneous operation. The delay that occurs causes the microcontroller to restart, losing it's operating process data before making the transition. Known temporary solution to this problem is to use a supercapacitor to fill the delay instantaneously, allowing the ATS to plug in the DC power from the battery without any delay. On the other hand, transitioning back from DC to AC is not problematic. It works as expected since the ATS can restore back it's AC power when it becomes available without losing any operational process data.

F. Data Logging Subsystem

The data logging subsystem functions to store data and enter it into the micro SD card via the micro SD card module. The form of the file created is a .txt because this type of file can be processed by the micro SD card module [22]. If the file is not on the micro SD card, the module will create it automatically [22]. The experiment began with a test run with submitted inputs. The data is subsequently stored to the micro SD card. After the operation, the micro SD card is unplugged and checked in a computer using a micro SD card reader.
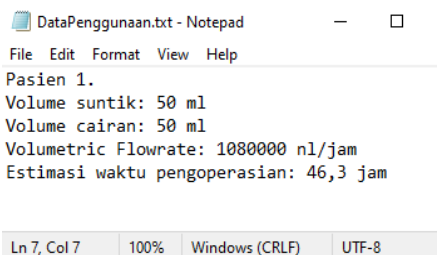

Fig. 10. A file named Usage Data stores the input data in .txt

The input data stored include the size of the injection volume used, the volume of drug liquid to be injected, the volumetric flow rate, and the estimated operating time of the injection, with the following formula:

$$Total\ time\ (hour) = \frac{Liquid\ volume\ (nl)}{Volumetric\ flowrate\ (\frac{nl}{hour})} \quad (5)$$

The standard injection sizes recommended by WHO are 20 cc, 50 cc, and 60 cc. The data logging subsystem successfully stores user input data that operates SPICAF. The micro SD card contains the DataUsage.txt file. The file contains data on the size of the injection, the volume of fluid entered, the input volumetric flow rate, and the estimated operating time obtained from the Total time calculation.

The data logging subsystem works by opening a file which is then filled in with data. After opening, the file must be closed again to end process for the file and ensure the module will save the data that has been inputted.

IV. CONCLUSION

Based on the results of testing and discussion, it can be concluded that the SPICAF system has been successfully built by WHO specifications and research feature targets. The bubble sensor subsystem successfully detects the air in the hose with the intensity of the light. The injection propulsion subsystem has succeeded in pushing the injection beyond the minimum specification with a soft starter implementation. The interface subsystem interacts with the user well. The notification subsystem can notify the user if an obstacle occurs with a specification of more than 45 dB. The data logging subsystem can store user input data.

The power manager subsystem can transition power from AC to DC and vice versa well, but for AC to DC, there is a delay so a supercapacitor is needed that can supply power instantly. In addition to the PMS solution, for future developments, a gear transmission method can be implemented in the gearbox to allow the working range of the SPICAF injection capability to be shifted. The fluid volume data is entered separately to allow the user to continue the rest of the drug that has not been injected or has failed. SPICAF can also be implemented with IoT (Internet of Things), such as data storage being saved directly to the user database, rather than stored in a micro SD card. For further development, it is necessary to do a real time test run of the injection process, since the accuracy measurement was performed using a different approach, which is reading it from the digital rotary encoder.

Since the development of SPICAF, the product has the specification capability to perform automatic data collecting, has backup power, can detect air through a bubble detector, can run a soft starter, has an alarm sound of more than 45 dB, and is capable of injection with a volume rate of 3600 nl. /hour up to 1080000 nl/hour.

REFERENCES

[1] Reynolds, R., Dennis, S., Hasan, I., Slewa, J., Chen, W., Tian, D., Bobba, S., & Zwar, N. (2018, January 9). A systematic review of chronic disease management interventions in primary care. *BMC Family Practice*, *19*(1). https://doi.org/10.1186/s12875-017-0692-3

[2] Shrestha, H., Bala, R., & Arora, S. (2014, May 19). Lipid-Based Drug Delivery Systems. *Journal of Pharmaceutics*, *2014*, 1–10. https://doi.org/10.1155/2014/801820

[3] Pardridge, W. M. (2012, August 29). Drug Transport across the Blood–Brain Barrier. Journal of Cerebral Blood Flow &Amp; Metabolism, 32(11), 1959–1972. https://doi.org/10.1038/jcbfm.2012.126

[4] U.S. Food & Drug Administration. (2018). *Infusion Pumps*. Available at: https://www.fda.gov/medical-devices/general-hospital-devices-and-supplies/infusion-pumps

[5] Jafarzadeh, M., & Farokhi, F. (2016, July). Design and construction of an automatic syringe injection pump. *Pacific Science Review A: Natural Science and Engineering*, *18*(2), 132–137. https://doi.org/10.1016/j.psra.2016.09.015

[6] Gorgich, E. A. C., Barfroshan, S., Ghoreishi, G., & Yaghoobi, M. (2015, December 18). Investigating the Causes of Medication Errors and Strategies to Prevention of Them from Nurses and Nursing Student Viewpoint. *Global Journal of Health Science*, *8*(8), 220. https://doi.org/10.5539/gjhs.v8n8p220

[7] Mirski, M., Lele, A., Fitzsimmons, L., Toung, T. K., & Warltier, D. (2007, January 1). Diagnosis and Treatment of Vascular Air Embolism. Anesthesiology, 106(1), 164–177. https://doi.org/10.1097/00000542-200701000-00026

[8] Malik, N., Claus, P. L., Illman, J. E., Kligerman, S. J., Moynagh, M. R., Levin, D. L., … Araoz, P. A. (2017). *Air embolism: diagnosis and management*. Future Cardiology, 13(4), 365–378. doi:10.2217/fca-2017-0015

[9] Hemauer, S. J., Kingeter, A. J., Han, X., Shotwell, M. S., Pandharipande, P. P., & Weavind, L. M. (2017, May). Daily Lowest Hemoglobin and Risk of Organ Dysfunctions in Critically Ill Patients. Critical Care Medicine, 45(5), e479–e484. https://doi.org/10.1097/ccm.0000000000002288

[10] Morrone, D., & Morrone, V. (2018). Acute Pulmonary Embolism: Focus on the Clinical Picture. *Korean Circulation Journal*, *48*(5), 365. https://doi.org/10.4070/kcj.2017.0314

[11] Flynn, F., Evanish, J. Q., Fernald, J. M., Hutchinson, D. E., & Lefaiver, C. (2016, August 1). Progressive Care Nurses Improving Patient Safety by Limiting Interruptions During Medication Administration. *Critical Care Nurse*, *36*(4), 19–35. https://doi.org/10.4037/ccn2016498

[12] Ahmed, M. G. A., Adam, A. B., Dennis, J. O., & Steele, G. S. (2009). Capacitor Device for Air Bubbles Monitoring. *International Journal of Electrical & Computer Sciences*, *9*(10), 93110–7878. https://doi.org/10.5281/zenodo.1056948

[13] Basjaruddin, N. C., Priyana, Y., & Kuspriyanto, K. (2013). Fault Tolerant Air Bubble Sensor using Triple Modular Redundancy Method. *TELKOMNIKA (Telecommunication Computing Electronics and Control)*, *11*(1), 71. https://doi.org/10.12928/telkomnika.v11i1.884

[14] World Health Organization. (2020). *COVID-19 Technical specifications for infusion devices*. WHO/2020-nCoV/MedDev/TS/InfDev. Available at: https://www.who.int/docs/default-source/medical-devices/tech-spec-infusion-devices-10072020-final-draft.pdf?sfvrsn=76f3e0fd_2

[15] Bolton, W. (2022, October 12). Mechatronics: Electronic Control Systems in Mechanical and Electrical Engineering (6th ed.). PEARSON INDIA.

[16] Musayev, E., & Karlik, S. E. (2003, December). A novel liquid level detection method and its implementation. Sensors and Actuators A: Physical, 109(1–2), 21–24. https://doi.org/10.1016/s0924-4247(03)00347-9

[17] ROHM Co. Ltd. (2014). *Digital 16bit Serial Output Type Ambient Light Sensor IC: BH1750*. https://components101.com/. Retrieved October 12, 2022, from https://components101.com/sites/default/files/component_datasheet/BH1750.pdf

[18] Changzhou Songyang Machinery & Electronics New Technic Institute. (2010, June 29). High Torque Hybrid Stepping Motor Specifications. Retrieved November 9, 2022, from https://components101.com/motors/nema17-stepper-motor

[19] Rotary Encoders. (2017). *Custom Raspberry Pi Interfaces*, 103–127. https://doi.org/10.1007/978-1-4842-2406-9_8

[20] Adafruit Industries. (2014, May 5). *All About Stepper Motors*. Adafruit Learning System. Retrieved October 13, 2022, from https://learn.adafruit.com/all-about-stepper-motors

[21] Alfariski, M. R., Dhandi, M., & Kiswantono, A. (2022, February 10). Automatic Transfer Switch (ATS) Using Arduino Uno, IoT-Based Relay and Monitoring. *JTECS : Jurnal Sistem Telekomunikasi Elektronika Sistem Kontrol Power Sistem Dan Komputer*, *2*(1), 1. https://doi.org/10.32503/jtecs.v2i1.2238

[22] Engineers, L. M. (2022, October 10). *Interfacing Micro SD Card Module with Arduino*. Last Minute Engineers. Retrieved October 12, 2022, from https://lastminuteengineers.com/arduino-micro-sd-card-module-tutorial/.